Sandia National Laboratories
Albuquerque, New Mexico 87185-0825

Date: October 4, 2005

To: Distribution

From: Ryan B. Bond, Org. 1515, MS 0825
Alfred A. Lorber, Org. 1541, MS 0382
Curtis C. Ober, Org. 1433, MS 0316

Subject : **Extension of Premo Capabilities to the Simulation of Flow in Chemical Equilibrium**

Accurate prediction of the aerothermal environment for hypersonic re-entry and cruise vehicles is essential for establishing design criteria for thermal protection systems. Accurate numerical predictions of such flight environments require that the effects of chemical reactions be taken into account. This chapter documents the effort to extend the capabilities of Premo, a computational fluid dynamics code which formerly used an ideal gas assumption, to include equilibrium chemistry modeling. This extension was accomplished through the development of a new C++ class hierarchy, GasProperties, to handle all calculations related to the thermodynamic state of the gas via different models, including ideal and equilibrium reacting gas. This new hierarchy was then implemented in Premo, replacing the old Gas_Props class which assumed an ideal gas. The test problems of a circular cylinder at various free stream Mach numbers demonstrated that the new GasProperties classes work properly for both ideal and equilibrium gases.

Introduction

Accurate prediction of aeroheating environments for re-entry vehicles via computational methods requires that those methods account for the effects of chemistry on the flow field. Assuming that the flow field behaves as an ideal gas results in a solution which may over-predict shock strength, shock standoff distance, and stagnation point heating. For simple geometries (*e.g.*, spherically-capped cones), the ideal gas assumption results in an overly conservative estimate of vehicle aeroheating. This, in turn, can lead to thermal protection system (TPS) designs that are heavier than they need to be for the actual flight environment. For complex geometries, the problem is much worse, since the locations of shock / shock and shock / boundary layer interactions may be inaccurately predicted when an ideal gas assumption is used. Because of this, the aeroheating may be under-predicted in regions where these interactions occur at real flight conditions, so aeroheating predictions by ideal gas methods are not guaranteed to provide conservative heating estimates.

The influence of chemical reactions on the flow field can be simplified with the assumption of local chemical and thermal equilibrium. However, this assumption is valid only if the characteristic time for chemical reactions is significantly smaller than the characteristic time for bulk fluid motion. Thus, the higher the free-stream velocity of the flow field, the more likely chemical non-equilibrium is to be a factor. At even higher speeds, the characteristic time for exchanges between internal energy states is significant relative to the characteristic time for bulk fluid motion, so thermal non-equilibrium effects become significant. This is especially true for low density flows when collisions between molecules happen less frequently, making the characteristic time for exchanges between internal energy states longer. In practice, the modeling approach

most appropriate for a given application will depend upon available resources, flight conditions, vehicle geometry, and the sensitivity of TPS design variables to the accuracy of aeroheating predictions.

Adding the equilibrium gas properties to Premo extended the simulation capabilities to high speed flows and aeroheating predictions while avoiding the expense of full finite-rate chemistry calculations. Although the code modifications will allow eventual extension to chemical and thermal non-equilibrium, the primary objective of this work was to provide a reacting gas capability which incorporated the assumption of chemical equilibrium. This was done in such a way as to preserve the performance of Premo for ideal gas cases as much as possible.

Background

Premo is a module of a larger multi-mechanics framework called SIERRA.[1] Premo is currently being developed as a production simulation tool to be used for analysis of compressible flows related to aerodynamic vehicle analysis and design. Flow regimes of interest range from transonic all the way up to hypersonic, both steady-state and transient. Premo is written in the C++ language and builds upon the object-oriented design of SIERRA to provide a flexible, maintainable, easy to use, and robust computational fluid dynamics (CFD) code package. The SIERRA framework provides data services for application modules which include I/O, domain decomposition and parallel process management, mesh adaptivity, load balancing, multiphysics code coupling, and nonlinear and linear solver libraries. Premo includes solvers for the Euler, Navier-Stokes, and Reynolds averaged Navier-Stokes governing equation sets.[2]

When mature, Premo is expected to replace some or all of the capabilities of currently-used Sandia codes. One such code is the Sandia Advanced Code for Compressible Aerothermodynamics Research and Analysis (SACCARA). SACCARA is based on PINCA, a distributed, parallel version of the commercial, finite-volume, Navier-Stokes code INCA from Amtec, Inc.[3,4,5] SACCARA has many of the physical models which now exist or are being developed in Premo. However, SACCARA is restricted to structured grid topologies and does not allow the multiphysics coupling that the SIERRA framework provides for Premo. SACCARA's solver is also quite slow for high Reynolds number flows, and no moving body capability exists with SACCARA. Premo will overcome some of these obstacles through its reliance on the SIERRA framework and through other research and development efforts. However, Premo's physical models must be extended beyond the ideal gas assumption to be applicable to the same sets of problems currently solved in SACCARA. The current effort is the first step at achieving that extension.

When medium fidelity aeroheating analyses are needed, the 2IT/SANDIAC/HIBLARG suite of engineering codes is frequently used. 2IT is an equilibrium gas, Euler (*i.e.*, inviscid) code capable of simulating flow fields around spherical geometries at all Mach numbers.[6] SANDIAC uses the same physical models as 2IT and is capable of simulating flow fields around analytically-defined geometries at high local Mach numbers (Mach 2 is generally considered to be the practical lower limit).[7] Together, these two codes can provide an inviscid flow field solution around spherically-capped, analytically-defined geometries at high free-stream Mach numbers. 2IT provides the portion of the solution around the stagnation region of the spherical cap, and SANDIAC provides the portion of the solution around the afterbody. This inviscid solution can then be used to provide the boundary layer edge conditions to HIBLARG, an equilibrium gas, integral boundary-layer code.[8] This 2IT/SANDIAG/HIBLARG approach is very fast and can be run for thousands of trajectory points in less than an hour. However, not all geometries of interest are spherically-capped (a restriction imposed by 2IT) or have analytically-defined afterbodies (a restriction imposed by SANDIAC). Also, SANDIAC is frequently unable to provide a reliable solution for vehicles at high angle-of-attack (for spherically-capped cones, the practical limit for angle-of-attack is approximately twice the half-angle of the cone). Since Premo is written as a general finite volume CFD code, it can be used to replace both 2IT and SANDIAC and provide the full Euler solution around general geometries, at all Mach numbers and angles-of-attack. This Euler solution can then be used to provide the boundary layer edge conditions to an integral boundary layer code. A parallel effort to update and generalize HIBLARG into a new code, SAPHIRE, is currently underway. Once this project is completed, the new equilibrium gas capability in Premo will allow Premo/SAPHIRE to replace 2IT/SANDIAC/HIBLARG for cases where 2IT/SANDIAC/HIBLARG can

not produce reliable results. This type of coupled analysis is not as accurate as full Navier-Stokes simulations in Premo, but Premo/SAPHIRE will be able to provide medium fidelity solutions far more quickly than full Navier-Stokes analysis. Thus, critical flight conditions can be analyzed for vehicle shape design using Premo's full Navier-Stokes capability, and TPS sizing for full trajectories can be performed in Premo/SAPHIRE.

Technical Approach

The chemical equilibrium assumption was implemented in Premo using a new C++ class hierarchy for handling all thermodynamic properties. The base class, called GasProperties, replaces the existing themodynamic properties class, called Gas_Props. Whereas Gas_Props used hard-coded ideal gas implementations for all of its functions, the GasProperties base class contains two derived classes, GasProperties_Ideal and GasProperties_Eq, the first of which assumes an ideal gas, and the second of which assumes more general thermodynamic properties represented by curve fits (including but not limited to models for equilibrium reacting gases). Other gas property options will be implemented by adding additional derived classes. Which derived class is used for a particular simulation is determined by user-specefied settings in the Premo input file. The new GasProperties_Ideal class contains all of the functionality of the old Gas_Props class, but it uses names that are consistent with the new GasProperties_Eq class. These functions are declared as pure-virtual in the base class GasProperties so that each flux, boundary condition, and initial condition function in Premo can be written generally, without regard to which derived classes will be instantiated for a particular execution of the code. The current interface may have to be extended further when derived classes supporting chemical and thermal non-equilibrium are added. However, the capabilities provided by the new GasProperties class will allow the frequent calculations of one thermodynamic variable from other thermodynamic variables to be easily extended for the more complex cases.

Equilibrium gas properties are determined from the physical models and bicubic spline fits of Liu and Vinokur.[9] The bicubic splines give pressure and temperature as functions of density and internal energy. The partial derivatives of pressure and temperature are assumed to be the partial derivatives of the bicubic splines. Bicubic splines have the property that they are continuous up to their second partial derivatives (C^2). This property makes them much better behaved numerically than curve fits that are only C^1 or C^0. Although some curve fits, such as the Tannehill curve fits, attempt to overcome these numerical problems with blending functions, they are still not as well behaved as curve fits that are naturally C^2.[10] These blending functions also frequently make use of transcendental functions, such as *exp(x)*, which are expensive to calculate. Additionally, the underlying physical models for the Liu and Vinokur fits are more accurate at higher temperatures and internal energies than the Tannehill fits. Since SACCARA's equilibrium gas capability relies on the Tannehill fits, Premo's newly developed equilibrium gas capability is expected to be more accurate from a physical standpoint and better behaved from a numerical standpoint.

Using these curve fits as definitions for pressure, temperature, and their derivatives, all thermodynamic properties needed for inviscid simulations can be easily calculated. The coefficients for the splines are stored in a table which is designed for speed and memory efficiency. For viscous simulations, models for viscous transport properties are also necessary. Although Liu and Vinokur do not provide physical models for the transport properties, models developed by others (such as Tannehill) can be fitted with the Liu and Vinokur style of splines. This enables the search algorithms implemented for the thermodynamic property spline coefficient databases to be used for searching the Liu and Vinokur formatted databases for viscous transport property spline coefficients. It also means that the curve fits which are used for the viscous transport properties will be C^2 like the thermodynamic curve fits. Although viscous transport properties have not yet been implemented, doing so is only a minor effort compared to the thermodynamic properties which have already been implemented and tested.

Although all of the flux function options have been converted to use the new GasProperties class, only the Steger-Warming[11] flux function has been extended to equilibrium reacting gas. Future work will focus on extending other flux function options in Premo to the more general equilibrium case. However, given the current options, Steger-Warming is the method of choice for high Mach number, inviscid flows, so it was the method chosen for extension to equilibrium as part of this effort. Future Premo development efforts may

involve the implementation of new flux routines such as modified Steger-Warming[12,13,14] or one of the AUSM/LDFSS family[15,16,17] of schemes.

For Steger-Warming calculations, several changes are necessary to the flux function.[18,19] These changes all collapse for the case of an ideal gas, so the modifications made to the existing Steger-Warming flux function implementation in Premo do not result in any changes to ideal gas solutions (this behavior was verified through an extensive set of regression tests that are part of the Premo code and test suite). Although these generalizations make ideal gas flux function calculations cost a few more floating point operations than the old, ideal-gas-specific formulations, this cost difference is expected to be insignificant.

An important part of code development is the construction of unit and regression tests for code features. Unit tests use stand-alone executables (as opposed to the primary code executable) that call only certain functions for testing. The two unit tests constructed as part of this work were a test which compares the output of all of the GasProperties_Ideal functions to the old Gas_Props functions and a test which compares GasProperties_Eq output to GasProperties_Ideal output when the coefficient table for the GasProperties_Eq curve fits is formulated to match ideal gas properties. These regression tests quickly found a number of design and coding errors early in the development process that could have manifested themselves as hard-to-find bugs in Premo, even though the simpler coefficient table did not test the full functionality of the GasProperties_Eq derived class.

The purpose of regression tests is to ensure that future changes to the code do not adversely affect current capabilities. As opposed to unit tests, regression tests generally involve executions of the primary code executable. The existing Premo regression tests allowed the integration of the new GasProperties class to take place while ensuring that these changes did not introduce errors which degraded formerly tested and verified functionality of the code. In addition to these tests, a new regression test was written to use the GasProperties_Eq derived class with the ideal gas coefficient table to make sure that future code changes did not adversely affect the equilibrium capability.

The principal test case for this work was a two-dimensional, circular cylinder in steady supersonic cross flow at various Mach numbers (2, 10, 15, 20 and 25). The cylinder radius was 0.5 meters, and the free stream values of temperature (T) and pressure (P) were representative of high altitude conditions (T = 227.89 K and P = 8.23501 Pa). The Mach 2 case was run with both the ideal gas and equilibrium reacting gas options in Premo for comparison. Since equilibrium air essentially behaves as an ideal gas for $T < 600$ K, the ideal and equilibrium cases were expected to produce very similar results. The higher Mach number cases were run with both equilibrium and ideal gas options in Premo as well as in SACCARA with the equilibrium option. Since SACCARA used the Tannehill curve fits for equilibrium air, its answers were expected to differ from Premo's, especially at higher free stream Mach numbers. However, the Premo versus SACCARA comparison was still useful given that the two were expected to be closer to each other than to the Premo ideal gas solutions. All of the calculations were performed with first-order settings for spatial accuracy in the codes. Other efforts currently underway are examining the performance of Premo for second-order settings on a Mach 3 blunt wedge. Once those efforts are completed, the performance of Premo with second-order settings for high Mach number equilibrium flows will be examined.

The grids used were analytically defined with the circular cross section of the cylinder as the inner surface and a hyperbola as the outer surface. The same physical dimensions were used for the high Mach number cases, but a much larger grid (in the physical space) was necessary to capture the shock for the Mach 2 runs (shock standoff distance (the distance along the stagnation line between the bow shock and the body) is inversely proportional to the Mach number). The grids all had 300 nodes along the surface of the cylinder and 100 nodes normal to the surface. The cylinder surface was modeled with a slip condition. The inflow boundary was modeled as supersonic inflow for SACCARA, but a Dirichlet boundary condition was used in Premo, rather than the Riemann-based supersonic inflow condition (both options exist in Premo, and they should give the same answer to within the tolerance of the Riemann solver's dissipation). The outflow boundaries were modeled as supersonic outflow boundaries for the high Mach number cases and as mixed subsonic/supersonic boundaries for the Mach 2 case. Figure 1 shows the computational domain with the boundaries labeled.

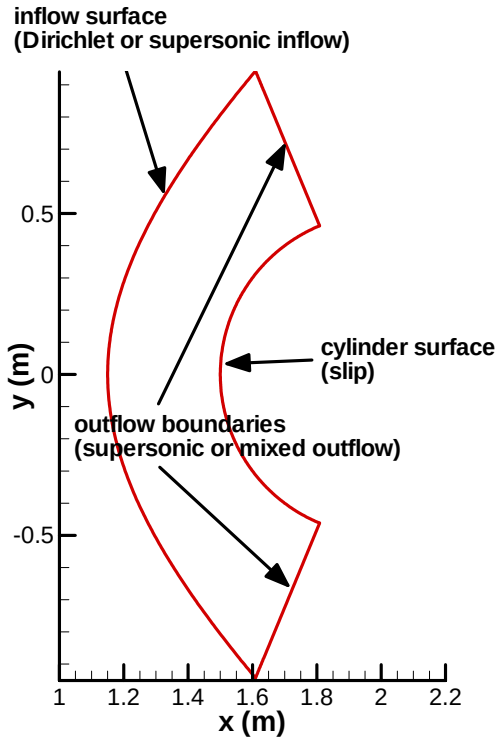

Figure 1 Domain with Boundaries Labeled

Results and Discussion

Mach 2 Case

Figure 2 shows the *T* and *P* profiles along the stagnation line for the Mach 2 case with both equilibrium gas and ideal gas in Premo. The solutions are very similar, although the equilibrium gas simulation predicts a *T* profile that is approximately 1% lower than the ideal gas simulation after the shock. This indicates that in the equilibrium gas simulation, either a very small portion of the internal energy is bound up as chemical energy or the unreacted gas is behaving in a calorically imperfect fashion. Although this would not be physically realistic near 400 K, the coefficient tables for the Liu and Vinokur curve fits were only generated to 1% accuracy. The 1% error in the curve fits accounts for the 1% difference in the solutions. The difference in *P*, which is representative of the other variables as well, is even smaller.

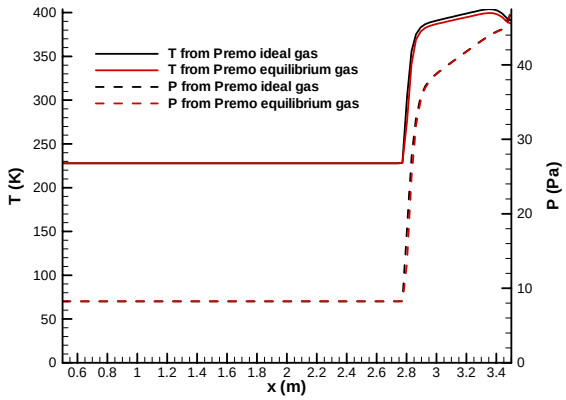

Figure 2 Stagnation Line *T* Profiles for Mach 2 Case

Mach 10 Case

Figure 3 shows the *H* contours for the Mach 10 case for ideal gas and equilibrium gas in Premo and for equilibrium gas in SACCARA. For the Premo solutions, drops of at least 8 orders of magnitude in the residual norms of each of the transport equations were achieved. However, probably because of the lack of smoothness in the Tannehill curve fits, drops of only 3 orders of magnitude were seen in the residual norms of each of the transport equations for the SACCARA solution. As can be seen in the plots, *H* is conserved throughout the solutions (as expected for an inviscid flow) except for slight variations caused by numerical dissipation in the vicinity of the shock wave, along the stagnation line, and near the slip surface. The much greater variance of *H* in the SACCARA solution is caused by additional eigenvalue smoothing beyond what is performed in Premo. The ideal gas solution in Premo shows slightly more dissipation of *H* in the vicinity of the shock than the equilibrium gas solution because the shock is stronger for the ideal gas case. (The grid is equally spaced in the circumferential and radial directions, so the observed difference in dissipation is strictly solution-dependent, rather than also being grid dependent..)

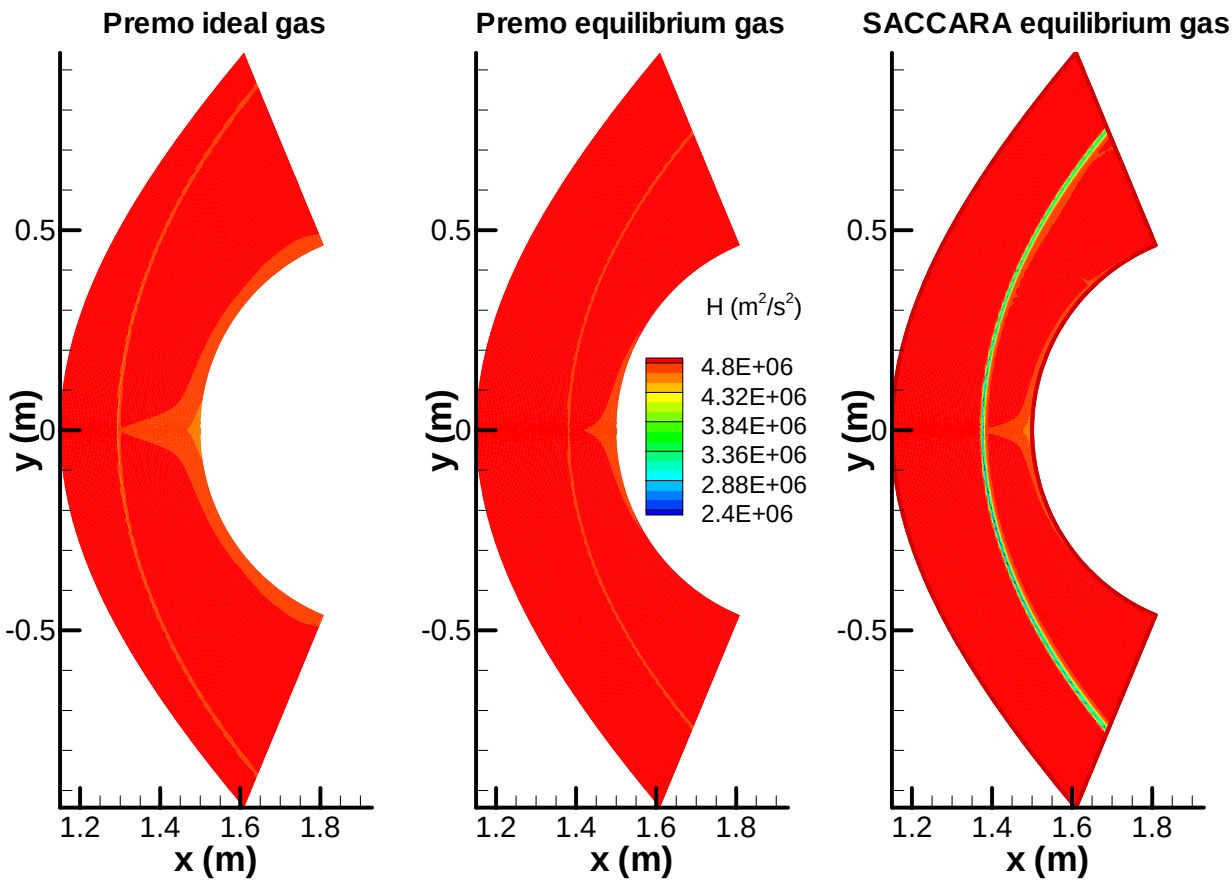

Figure 3 *H* Contours for Mach 10 Case

Figure 4 shows the *T* contours for all three Mach 10 solutions. The differences between ideal and equilibrium gas computations are apparent in this plot. As expected, *T* is much lower behind the shock in the equilibrium solutions than in the ideal solution. This is because much of the internal energy (e) is bound up as chemical energy rather than the thermal energy states on which *T* depends. Despite logarithmic scaling which accentuates variances on the lower end of the temperature scale, the contour range required for the ideal solution makes the two equilibrium solutions nearly indistinguishable. Figure 5 shows a plot of temperature along the stagnation line for the three solutions. In this solution, the only difference between the Premo and SACCARA equilibrium solutions appears to be the shock standoff distance, with Premo predicting the shock closer to the cylinder than SACCARA does.

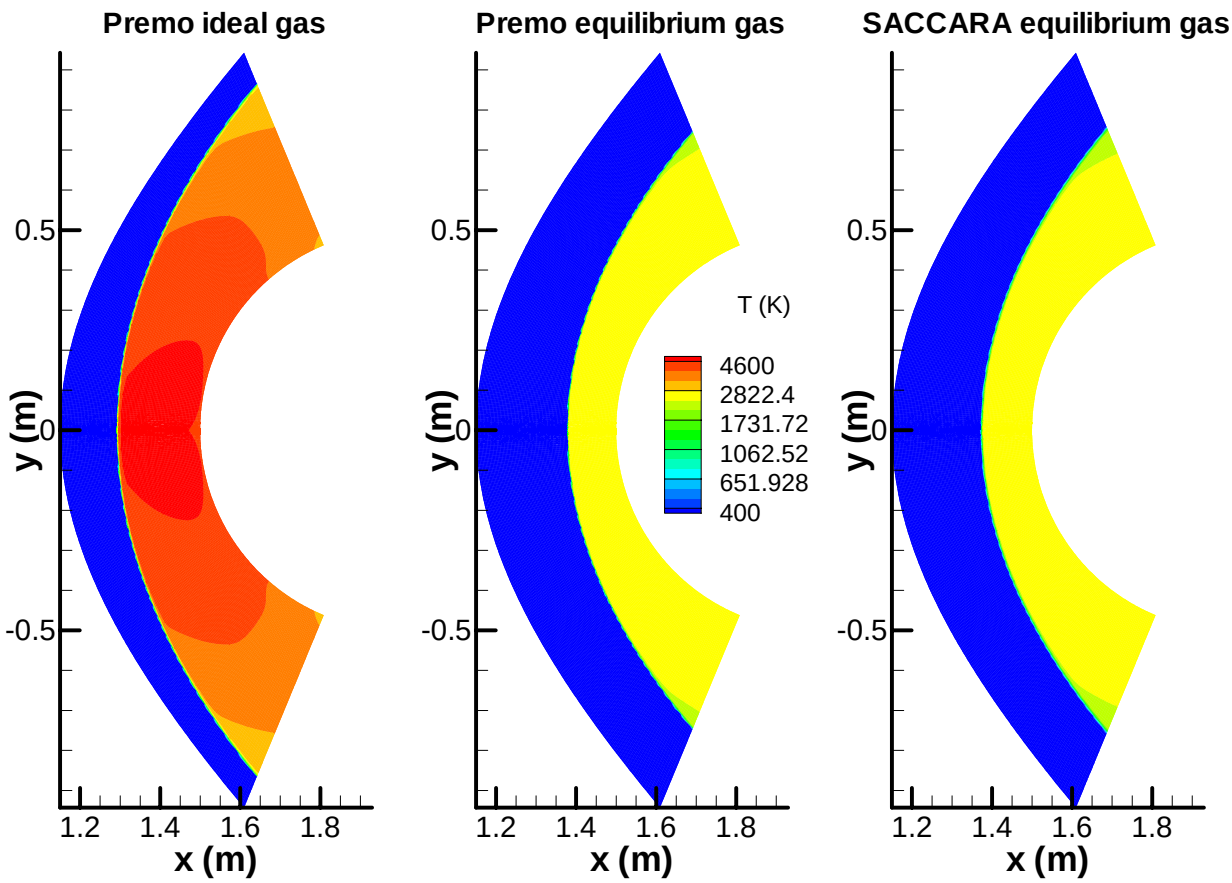

Figure 4 ***T*** **Contours for Mach 10 Case**

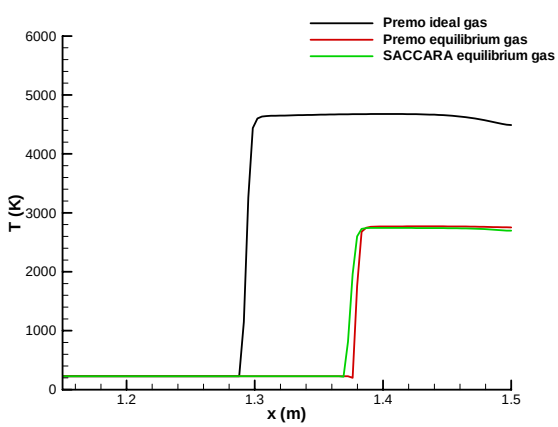

Figure 5 **Stagnation Line** ***T*** **Profiles for Mach 10 Case**

This discrepancy is a result of the omission of the inhomogeneous flux term (one of the modifications to Steger-Warming for thermally imperfect gases) from SACCARA. The inhomogeneous flux term, *F'*, arises because the flux function, *F(U)*, is not homogeneous for a thermally imperfect gas:

$$\boldsymbol{F(U) = \frac{\partial F}{\partial U} U + F'}$$

where

$$\boldsymbol{F} = \begin{bmatrix} \rho\vec{V} \\ \rho\vec{V}\otimes\vec{V} + p\vec{\vec{I}} \\ \rho\vec{V}H \end{bmatrix} \qquad \boldsymbol{U} = \begin{bmatrix} \rho \\ \rho\vec{V} \\ \rho E \end{bmatrix} \qquad \boldsymbol{F}' = -\begin{bmatrix} 0 \\ (\gamma - 1 - \kappa)p\vec{\vec{I}} \\ (\gamma - 1 - \kappa)p\vec{V} \end{bmatrix}$$

$$\gamma = \frac{\rho c^2}{p} \qquad \kappa = \left.\frac{\partial p}{\partial(\rho e)}\right|_{\rho}$$

At one point in the development of the Steger-Warming modifications in Premo, confusion arose as to the sign of the inhomogeneous portion of the flux because a paper by Liou, van Leer, and Shuen disagreed with references 18 and 19.[20] Algebraic manipulations of the terms eventually confirmed that references 18 and 19 were correct, but in the interim, an experiment was done with the Mach 10 case to compare the solutions obtained with positive and negative signs in front of the inhomogeneous portion of the flux. As can be seen in Figure 6, the shock in the SACCARA solution lies right between those of the two Premo solutions. Because of this, suspicion arose that the inhomogeneous portion of the flux had been omitted from SACCARA. Examination of the SACCARA source code confirmed this suspicion, so the SACCARA and Premo solutions should be expected to differ to the extent that thermally imperfect behavior of the gas is significant.

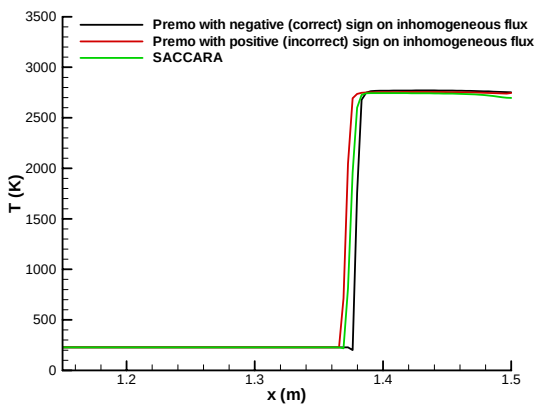

Figure 6 Stagnation Line *T* Profiles for Flux Comparison

Mach 15 Case

For the Mach 15 case, the ideal gas run in Premo and equilibrium gas run in SACCARA were able to achieve 8 and 3 orders of magnitude convergence, respectively, in the residual norms, just as in the Mach 10 runs. However, the equilibrium gas run in Premo achieved 6 orders of magnitude convergence in the residual norms for the Mach 15 run, whereas 8 orders of magnitude of convergence were possible for the Mach 10 case. Figure 7 shows the *H* contours for the three Mach 15 solutions. Although the levels are different than for the Mach 10 case, the constancy in *H* is evident for all three solutions, just as it was for the Mach 10 case. Once again, SACCARA shows higher levels of dissipation near the shock.

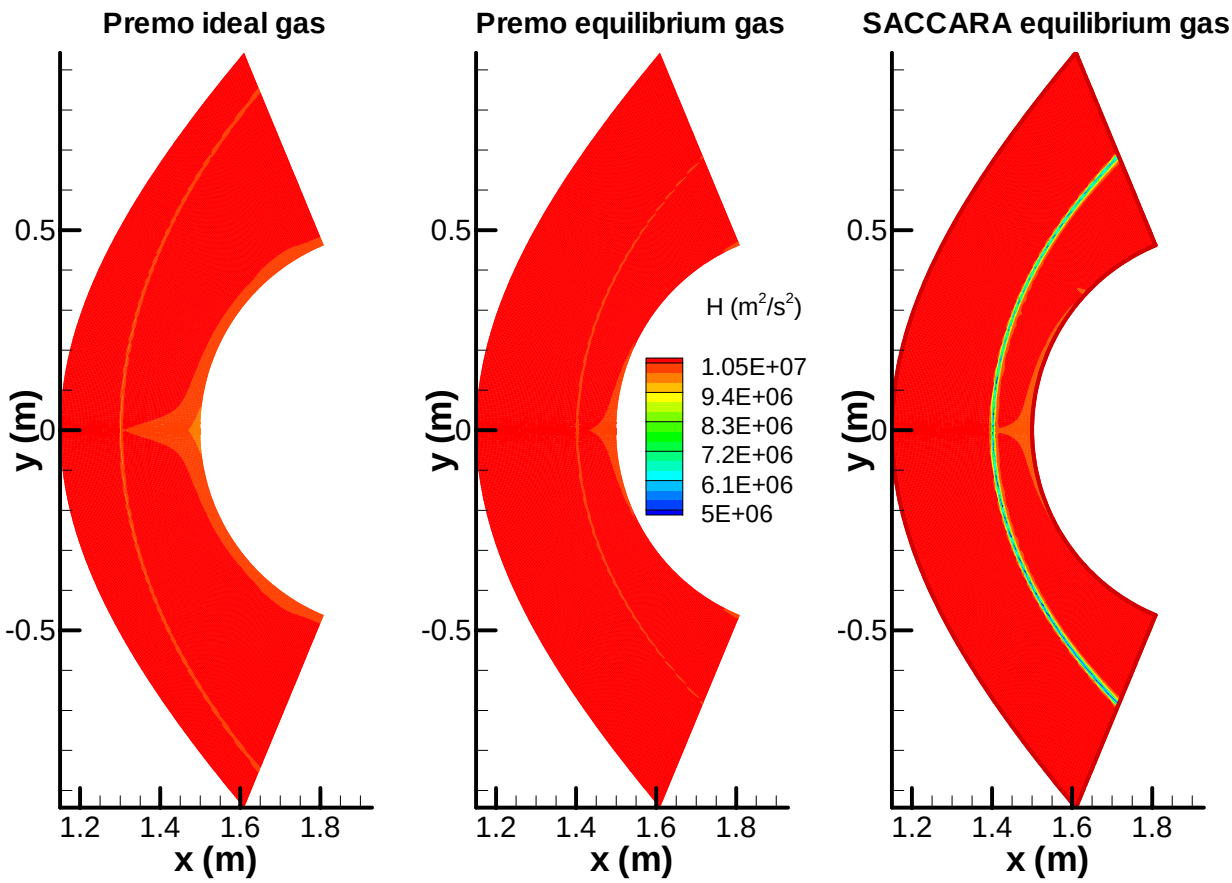

Figure 7 *H* Contours for Mach 15 Case

Figure 8 shows that at this higher Mach number, the equilibrium solutions for Premo and SACCARA exhibit differences in *T* in the stagnation region. This is most likely a result of the different gas property models (Liu and Vinokur versus Tannehill) between the two codes, rather than a result of the missing inhomogeneous flux in SACCARA. Because the Tannehill curve fits are not as accurate at higher temperatures, differences in the *T* distrbutions aft of the shock appear at Mach 15 that did not appear at Mach 10. Figure 9 shows the *T* profile along the stagnation line for all three solutions. In addition to predicting a higher *T* in the stagnation region, the equilibrium gas run in Premo also predicts a slightly smaller shock standoff distance, just as for the Mach 10 case, likely because of the missing inhomogeneous flux in SACCARA.

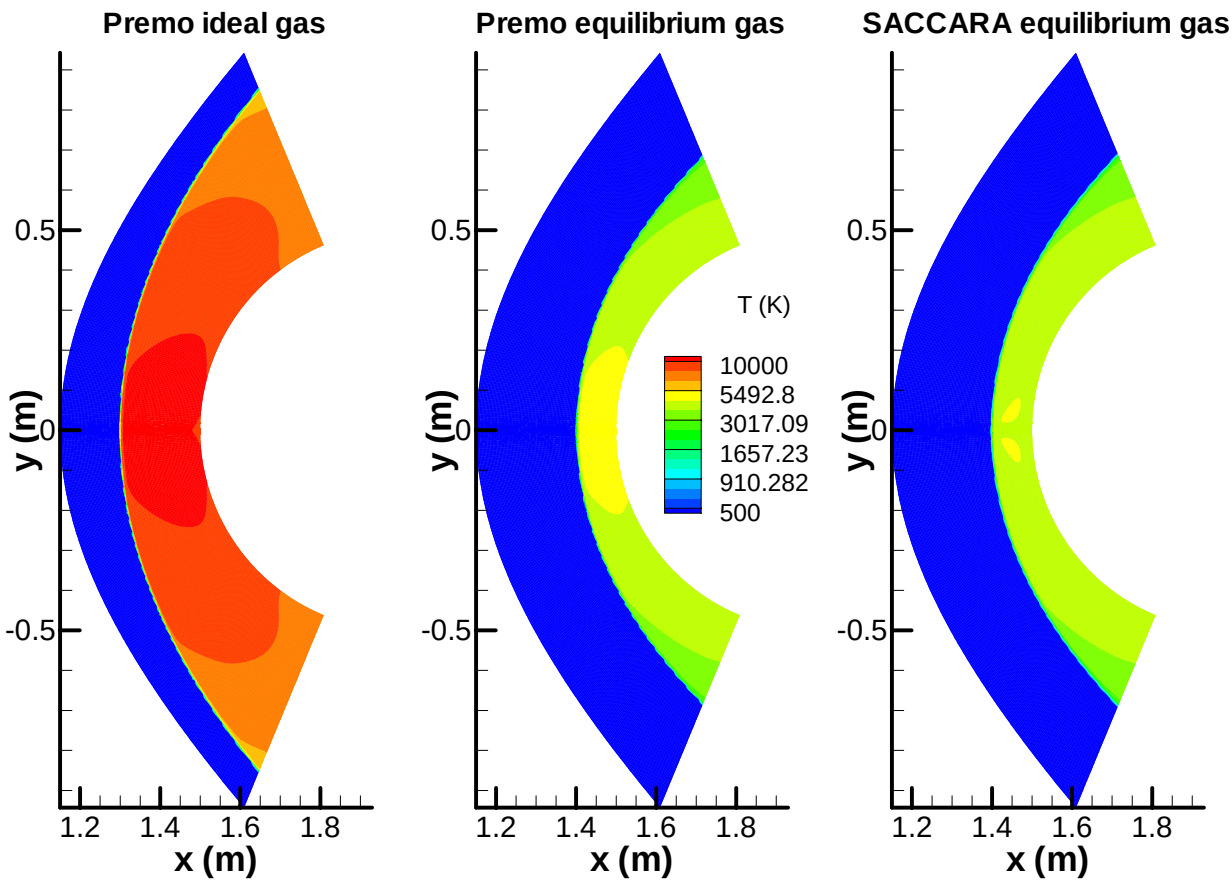

Figure 8 ***T*** **Contours for Mach 15 Case**

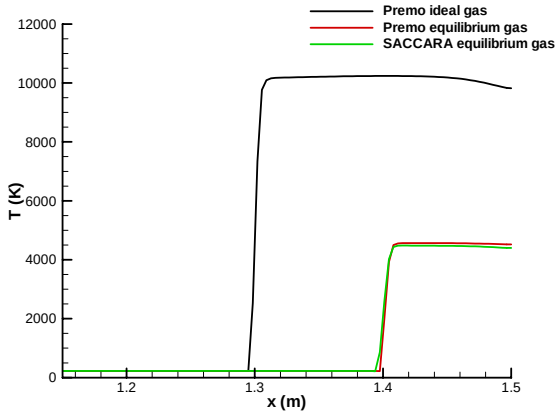

Figure 9 **Stagnation Line** ***T*** **Profiles for Mach 15 Case**

Mach 20 and 25 Cases

Since the iterative convergence limit of the equilibrium gas Premo run was not as good as the ideal gas Premo run for the Mach 15 case, and since solutions at Mach 20 and above were not obtainable for equilibrium gas Premo, examination into the behavior of the inhomogeneous portion of the flux began. References 18 and

19 do not make suggestions for how to difference the inhomogeneous flux. Reference 20 suggests central differencing based upon experience, so that was used in Premo up through the Mach 15 case. However, since Reference 20 had a sign error on the inhomogeneous term, the experience mentioned is probably not relevant. Since the term is inhomogeneous, it is not possible to do an eigenvalue splitting such as the Steger-Warming splitting that is used for the homogeneous portion of the flux. Instead, the following van Leer type splitting was used:

$$\boldsymbol{F'} = \boldsymbol{F'^{+}_{L}} + \boldsymbol{F'^{-}_{R}}$$

where

$$\boldsymbol{F'^{\pm}} = \boldsymbol{D^{\pm}_{\mathrm{vL}}}\boldsymbol{F'}$$

$$\boldsymbol{D^{\pm}_{\mathrm{vL}}} = \tfrac{1}{4}\left(\hat{\boldsymbol{M}}_{1/2} \pm 1\right)^{2}\left(2 \mp \hat{\boldsymbol{M}}_{1/2}\right)$$

$$\hat{\boldsymbol{M}} = \max\left(-1, \min\left(1, \boldsymbol{M}\right)\right)$$

and $M_{1/2}$ is the interface Mach number, $(M_L+M_R)/2$. This splitting for the inhomogeneous portion of the flux was used for the Mach 20 and 25 cases.

Figure 10 shows the T contours for the Mach 20 runs, and Figure 11 shows the T profiles along the stagnation line. As in the Mach 15 case, the Premo and SACCARA equilibrium gas solutions differ slightly in shock standoff distance (Premo's predicted distance is shorter than SACCARA's) and T profile on the stagnation line (Premo's predicted T profile aft of the shock is higher than SACCARA's). With the change from central to van Leer splitting on the inhomogeneous portion of the flux, 8 orders of magnitude of iterative convergence are possible for the equilibrium gas run in Premo. (No convergence is possible at all for the higher Mach number runs with central differencing.) The same convergence trends and differences between Premo and SACCARA exist for the Mach 25 results, shown in Figure 12 and Figure 13.

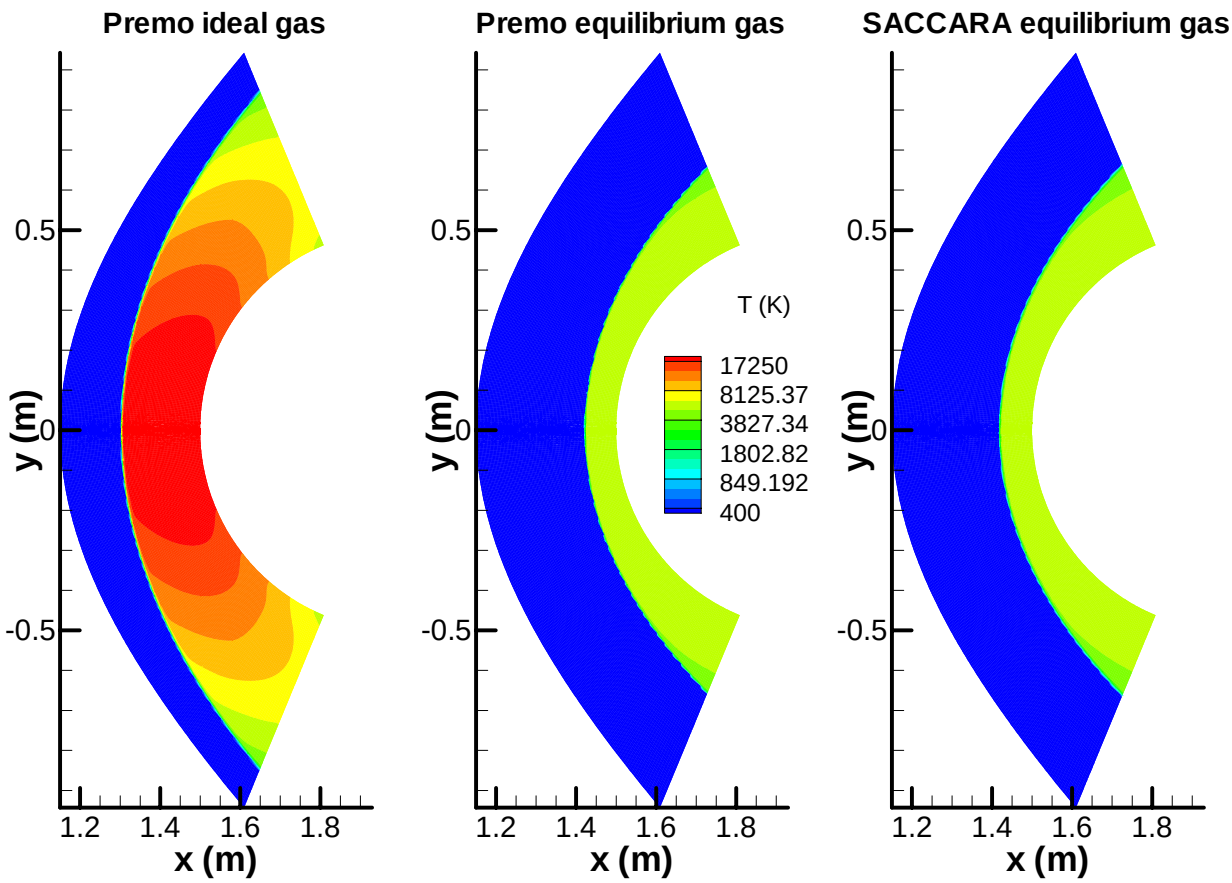

Figure 10 ***T*** **Contours for Mach 20 Case**

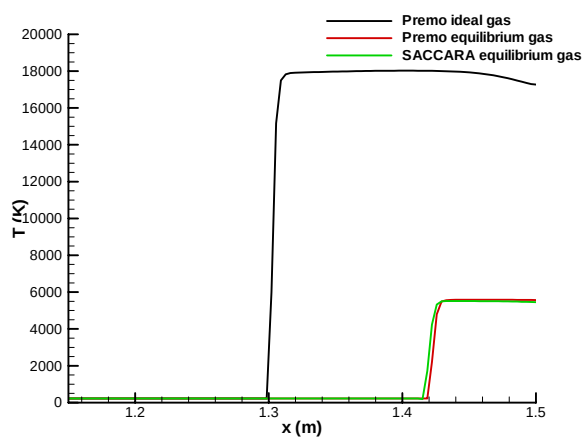

Figure 11 **Stagnation Line** ***T*** **Profiles for Mach 20 Case**

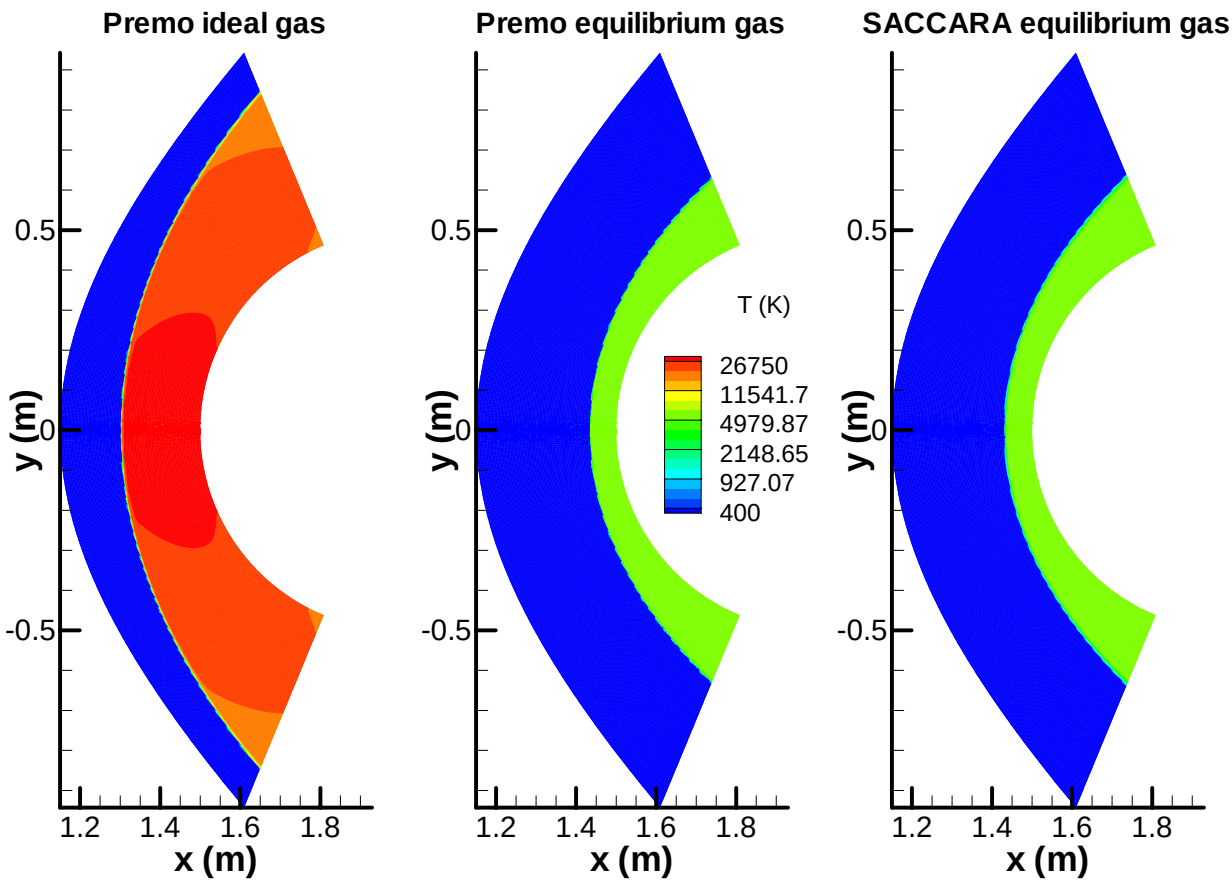

Figure 12 ***T*** **Contours for Mach 25 Case**

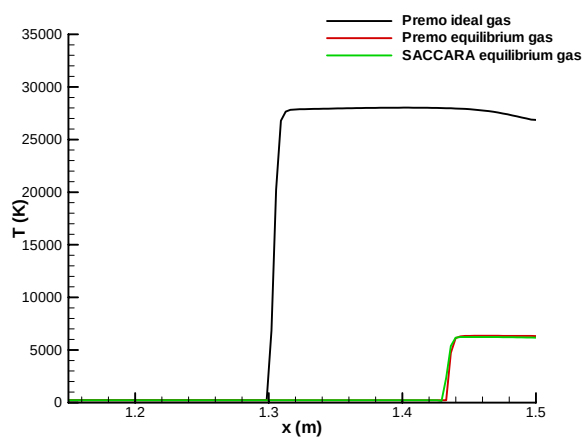

Figure 13 **Stagnation Line** ***T*** **Profiles for Mach 25 Case**

Conclusions

Results presented demonstrate proper functionality of the new equilibrium reacting gas capability for Premo. The equilibrium solution matches the ideal gas solution to the extent expected for a Mach 2 flow over a

circular cylinder. Equivalency to within the accuracy of the equilibrium curve fits demonstrates that the ideal gas solution is recovered by the equilibrium modeling technique for this low temperature range. At Mach 10, only a slight difference in the shock standoff distance exists between the Premo and SACCARA equilibrium gas solutions. Comparison of solutions and examination of the SACCARA source show this discrepancy to be the result of SACCARA's omission of a portion of the flux needed for thermally imperfect gas simulations. At higher Mach numbers (15, 20, and 25), the temperature of the equilibrium solutions in the stagnation region is such that the Premo and SACCARA simulations differ more than at Mach 10, likely because of differences at higher T in the curve fits upon which their equilibrium gas modeling capabilities are based.

Future Work

Future work will include the calculation of viscous transport properties for an equilibrium gas so that viscous flows can be simulated. Additionally, examination of Premo's performance with second-order settings for spatial accuracy for this class of flows will commence one the current behavior is understood and acceptable for lower Mach number flows. Subsequently, Premo will be extended to handle flows in chemical non-equilibrium and, eventually, thermal non-equilibrium as well.

Acknowledgments

The authors would like to thank Tom Smith for his assistance in developing the test problems for Premo and for his assistance in debugging the GasProperties_Eq functions. They would also like to thank Matt Barone for his help in setting up the test cases for SACCARA. They would also like to thank Fred Blottner for his assistance and the use of his codes in generating the coefficient tables for the Liu and Vinokur equilibrium curve fits.

References

[1] Edwards, H. C. and Stewart, J. R., "SIERRA: A Software Environment for Developing Complex Multiphysics Applications," Proceedings of First MIT Conference on Computational Fluid and Solid Mechanics, Elsevier Scientific, K. J. Bathe, ed., June 2001.
[2] Smith, T. M., Ober, C. C., and Lorber, A. A., "SIERRA/Premo—A New General Purpose Compressible Flow Simulation Code," AIAA Paper 2002-3292, June 2002.
[3] Wong, C. C., Soetrisno, M., Blottner, F. G., Imlay, S. T., and Payne, J. L., "PINCA: A Scalable Parallel Program for Compressible Gas Dynamics with Non-equilibrium Chemistry," SAND 94-2436, Sandia National Laboratories, Albuquerque, NM, 1995.
[4] Wong, C. C., Blottner, F. G., Payne, J. L., and Soetrisno, M., "Implementation of a Parallel Algorithm for Thermo-Chemical Nonequilibrium Flow Solutions," AIAA Paper 95-0152, January 1995.
[5] *INCA User's Manual, Version 2.0*, Amtec Engineering, Inc., Bellevue, WA, 1995.
[6] Brant, D., Wade, M., and Morgan, J., "Computational Technique for Three-Dimensional Inviscid Flow Fields About Re-Entry Vehicles: Vol. II User's Manual," SAMSO TR-79-5, General Electric Company, Philadelphia, PA, 1978.
[7] Noack, R. W., and Lopez, A. R., "Inviscid Flow Field Analysis of Complex Reentry Vehicles: Volume I, Description of Numerical Methods," SAND 87-0776/1, Sandia National Laboratories, Albuquerque, NM, 1988.
[8] Polansky, G. F., "Hypersonic Integral Boundary Layer Analysis of Reentry Geometries (HIBLARG) Code Description and User's Manual Version 2.0," SAND 89-0552, Sandia National Laboratories, Albuquerque, NM, 1990.
[9] Liu, Y. and Vinokur, M., "Equilibrium Gas Flow Computations. I. Accurate and Efficient Calculation of Equilibrium Gas Properties," AIAA Paper 89-1736, June 1989.
[10] Srinivasan, S., Tannehill, J. C., and Weilmuenster, K. J., "Simplified Curve Fits for the Thermodynamic Properties of Equilibrium Air," NASA Reference Publication 1181, 1987.

[11] Steger, J. L. and Warming, R. F., "Flux Vector Splitting of the Invsicid Gasdynamic Equations with Applications to Finite Difference Methods," *Journal of Computational Physics*, vol. 40, no. 2, pp. 263-293, 1981.
[12] MacCormack, R. W. and Candler, G. V., "The Solution of the Navier-Stokes Equatiosn Using Gauss-Seidel Line Relaxation," *Computers and Fluids*, vol. 17, no. 1, pp. 135-150, 1989.
[13] Campbell, C. H. and Candler, G. V., "A Flux Consistent Implementation of Flux Vector Splitting, " AIAA Paper 2004-0243, January 2004.
[14] Druguet, M.-C., Candler, G. V., and Nompelis, I., "Effects of Numerics on Navier-Stokes Computations of Steady Hypersonic Double-Cone Flows," *AIAA Journal*, vol. 43, no. 3, pp. 616-623, 2005.
[15] Wada, Y. and Liou, M.-S., "A Flux Splitting Scheme with High-Resolution and Robustness for Discontinuities," AIAA Paper 94-0083, January 1994.
[16] Liou, M.-S., "Progress Towards an Improved CFD Method: AUSM+," AIAA Paper 95-1701, June 1995.
[17] Edwards, J. R., "A Low-Diffusion Flux-Splitting Scheme for Navier-Stokes Calculations," *Computers and Fluids*, vol. 26, no. 6, pp. 635-659, 1997.
[18] Vinokur, M. and Liu, Y., "Equilibrium Gas Flow Computations II: An Analysis of Numerical Formulations of Conservation Laws," AIAA Paper 88-0127, January 1988.
[19] Vinokur, M. and Montagne, J.-L., "Generalized Flux-Vector Splitting and Roe Average for an Equilibrium Real Gas," *Journal of Computational Physics*, vol. 89, no. 2, pp. 276-300, 1990.
[20] Liou, M.-S., van Leer, B., and Shuen, J.-S., "Splitting of Inviscid Fluxes for Real Gases," *Journal of Computational Physics*, vol. 87, no. 1, pp. 1-24, 1990.

Distribution

MS 0316	1420	Sudip Dosanjh
MS 0316	1433	Jim Strickland
MS 0316	1416	Russell Hooper
MS 0316	1433	Tom Smith
MS 0321	1400	Bill Camp
MS 0321	1430	Jennifer Nelson
MS 0382	1541	Steve Gianoulakis
MS 0382	1543	Jim Stewart
MS 0382	1541	Stefan Domino
MS 0382	1543	Carter Edwards
MS 0382	1541	Jeff Fisher
MS 0384	1500	Art Ratzel
MS 0384	1540	Hal Morgan
MS 0821	1530	Anthony Thornton
MS 0821	1532	Lou Gritzo
MS 0824	1510	Wahid Hermina
MS 0825	1515	Basil Hassan
MS 0825	1515	Matt Barone
MS 0825	1515	Fred Blottner
MS 0825	1515	Larry Dechant
MS 0825	1515	Jeff Payne
MS 0825	1515	Don Potter
MS 0825	1515	Justin Smith
MS 0826	1513	Michail Gallis
MS 0834	1512	Justine Johannes
MS 0836	1516	Gene Hertel
MS 0847	1520	Pete Wilson
MS 1135	1532	John Hewson
MS 1135	1532	Sheldon Tieszen
MS 1158	5424	Ken Chavez
MS 1158	5424	Gary Polansky
MS 1162	5422	Walt Rutledge
MS 1162	5422	Mary McWherter-Payne
MS 1162	5422	Mike Macha
MS 1310	1513	Steve Kempka
MS 9409	8775	Chris Moen